Adsorption (2014) 20:777–788
DOI 10.1007/s10450-014-9621-0

Effect of electrostatic properties of IRMOFs on VOCs adsorption: a density functional theory study

Ying Wu · Defei Liu · Yongbiao Wu · Yu Qian · Hongxia Xi

Received: 1 January 2014 / Revised: 13 May 2014 / Accepted: 18 June 2014 / Published online: 28 June 2014

Abstract Metal–organic frameworks (MOFs) are of great promises for the adsorption of volatile organic compounds (VOCs). The adsorption of methanol, aldehyde and one on IRMOF-1 and an amino-functionalized framework, IR-MOF-NH_2, were investigated by density functional theory. The adsorption mechanisms and the effects of amino functionalization were clarified with comparison of binding energies, optimized configurations, atomic partial charges and the electrostatic potentials. The calculated results revealed that the electron-donating effect of amino groups had great influence on the electrostatic properties of the framework. The adsorption of methanol was greatly enhanced on organic linkers of IRMOF-NH_2 compared to IRMOF-1, but weakened on the metal corners, different from the adsorption behaviors of aldehyde and acetone. A plausible interaction mechanism was inferred as the VOCs adsorption might be governed by the electrostatic interaction between methyl groups of the adsorbates and the binding sites of the framework, while the polar groups of adsorbates only interacted with framework through weak interaction like H-bonding. Besides, the steric hindrance effects of the inserted amino groups should also be taken into consideration, depending on the configuration and the electrostatic properties of the adsorbates. The binding mechanisms of VOCs on IRMOF-1 and IRMOF-NH_2, provide fundamental insights into the oriented design of MOFs for the adsorption of VOCs.

Y. Wu · D. Liu · Y. Wu · Y. Qian · H. Xi (✉)
The School of Chemistry and Chemical Engineering,
South China University of Technology,
Guangzhou 510641, Guangdong, People's Republic of China
e-mail: cehxxi@scut.edu.cn

Keywords Density functional theory · Metal–organic framework · Adsorption · VOCs · Binding energies

1 Introduction

Volatile organic compounds (VOCs) are a set of major air pollutants in the upper troposphere, including methanol, aldehyde and ketone (Su et al. 2013) etc., which are not only considered as harmful compounds to health (Wolkoff 2013), but also induces some serious environmental problems, e.g. the photochemical smog, destruction of ozone layer (Laaksonen et al. 1997). Hence the development of novel technologies for VOCs treatment have triggered increasing attention to comply with the environmental regulations. Among various technologies for removing VOCs, adsorption has been generally considered as one of the most effective strategy as its industrial maturity and no chemical degradation (Dou et al. 2011). Hence, experimental and theoretical studies have increasingly focused on the adsorption of VOCs on various porous materials such as activated carbon (AC) (Xuemin et al. 2011), AC fiber (Le Cloirec 2012) and zeolite (Kim and Ahn 2012) etc., however their pore blocking and lack of regeneration ability of these materials prevent them from industrial application of adsorbing VOCs.

Metal–organic frameworks (MOFs) (Lin et al. 2012), as known as a new family of coordination polymers, are a set of regular crystalline solids with well-organized structures constructed by the coordination of metal corners with organic linkers. MOFs are known for their well-defined porosity, high surface area, adjustable pore geometry and chemical functionality (Furukawa et al. 2013), which are recognized as the potential alternatives in VOCs capture. Montoro et al. (2011) reported a novel MOF-5 type

framework to adsorb VOCs even in ambient moisture, and proposed the VOC-MOF interaction was dominated by pore size and surface hydrophobicity rather than the unsaturated metal sites. Luebbers et al. (2010) experimentally examined the adsorption of over 30 VOCs on IRMOF-1, indicating great intensification of the binding energies (BEs) by the structural degradation of the frameworks, but lack of thermodynamic interaction on organic linkers. Nevertheless, the direct observation of VOCs on the preferential adsorption sites of MOFs remains a challenging and time-consuming task, and the unclarified structure–property relationship of newly-constructed MOFs may impede their developments and applications for VOCs adsorption.

As a result, experimental studies are expected to be complemented by computational simulations. In the computational studies of gas adsorption, the positions of adsorbates are usually adjusted to find the most favorable conformation so as to investigate the preferential adsorption sites of MOFs as well as their performance for specific applications (i.e. VOCs adsorption/separations). In these cases, the refinements of adsorbate-adsorbent complexes are commonly obtained by geometric optimization, and the binding energy calculations are further carried out to clarify the interaction strength. Molecular dynamics (MD) simulation is known as a rapid method for geometric optimization. Since the electronic charges used for describing electrostatic interactions are usually kept static, the MD simulations is allowed to refine the configurations on very large MOFs systems [e.g. MIL-101 (Hu et al. 2013)]. However, the final quality of MD optimization significantly depends on the force fields adopted in the calculations. Since developing accurate and transferable forcefields are extremely challenging (Fang et al. 2014), general forcefields [e.g. UFF (Rappe et al. 1992), Dreiding (Mayo et al. 1990)] are still the most widely used in the recent studies, but they are less reliable to describe the more complex adsorption systems. In addition to MD simulation, density functional theory (DFT) method (Cicmanec et al. 2013; Yang et al. 2013) gives another way to theoretically obtain the geometric equilibrium of MOF-based adsorption systems. Contrary to MD simulations, DFT procedure is an electronic ground-state theory that defines the energy of atoms at prescribed positions from corresponding electron density (Young 2004). By using either localized or delocalized basis functions, DFT method allows great efficiency in geometric optimization. Although DFT approach is more time-consuming than MD simulations, it has been considered to be more capable of providing predictions with a satisfactory trade-off between accuracy and speed, and widely employed in studying both homogeneous (Liang et al. 2009) and heterogeneous (Liu et al. 2011) systems.

To date, DFT-based computational studies on various functionalities of MOFs have showed potential applications in gas storage/separation (Wu et al. 2014a; Zhang et al. 2013), and the ligand amino-functionalizations on MOFs are also observed to have benefits on gas adsorption. Torrisi et al. (2013) implied the amino-modification of MIL-53 enhanced the adsorption affinity for CO_2, by introducing additional binding sites at low pressure. Yang et al. (2011) further suggested amino-introduction to have great intensification on the thermodynamic selectivity of CO_2 from CH_4 and N_2 over UiO-66(Zr). However, the negative steric effect of introduced amino groups also shows a drawback to the adsorption performance. Devautour-Vinot et al. (2012) indicated the significant reduction of the ligand dynamics of UiO-66(Zr) by amino groups, which might suppress the diffusion rate of guest molecules. Leus et al. (2012) also reported the amination did not give rise to an increased CO_2 capacity or CH_4/CO_2 selectivity on MIL-47. Although many works were concentrated on gases adsorption over amino-modified MOFs, little attention has been paid to the adsorption of VOCs. As a subfamily of MOFs, the isoreticular metal–organic frameworks (IRMOFs) are considered as attractive candidates for VOC adsorption (Montoro et al. 2011; Luebbers et al. 2010) because of their high surface area (500–4,500 m^2/g) and free volume (55.8–91.1 %) (Eddaoudi et al. 2002; Ferey et al. 2005). However, works on IRMOFs are mainly focus on the synthesis, characterization and the adsorption application of N_2, CO_2, CH_4, H_2, etc. (Ford et al. 2009; Babarao et al. 2007), but the simulation studies about the adsorption mechanisms of VOCs on IRMOFs are still limited in the literatures. Moreover, amino-functionality effects of IRMOFs on VOCs adsorption also remain uncertain.

In this paper, DFT calculations were carried out for investigating the adsorption mechanisms of methanol, aldehyde and acetone on IRMOF-1 and an amino-functionalized framework, IRMOF-NH_2. The selected VOCs with varied electrostatic properties were expected to give a distinction of adsorption behaviors. Geometric optimization was performed to search the binding sites of the frameworks, following by the BEs calculations of the selected configurations so as to indicate the interaction strength between adsorbate-adsorbent complexes. Finally, the effects of amino-functionalization on VOCs adsorption were clarified by comparing the BEs of different energy-minimum configurations, and the electrostatic potentials (ESPs) of the parent and functionalized IRMOFs.

2 Models and computational details

2.1 Structures construction

IRMOF-1, also known as MOF-5 (Yaghi et al. 2003), has a *Fm-3m* crystal space group with a lattice constant of

25.832 Å, a crystal density of 0.593 g/cm^3 and a free volume of 79.2 % (Eddaoudi et al. 2002). For simulation, the crystal structure of the framework was taken from experimental X-ray diffraction data (Eddaoudi et al. 2002), as shown in Fig. 1a. IRMOF-1 was a 3-dimensional (3D) porous cubic framework that constructed with eight metal-oxide corners of Zn_4O connected by twelve 1,4-benzene-dicarboxylate (BDC) organic linkers. Since the varied inclination angle of BDC linkers in the structure, the pores were divided into small and big cells, denoted as S and B in Fig. 1b, respectively. On the other hand, IRMOF-NH_2 was constructed on the basis of its parent IRMOF-1, with the H atoms of BDC organic linker symmetrically replaced by four $–NH_2$ groups, which was expected to prevent the textural non-symmetry effects for adsorption interactions, as denoted in Fig. 2. This version of amino functionality was reported by Mu et al. (2010), suggesting the introduction of $–NH_2$ groups could verify the pore size and electron-combining properties of IRMOFs, but retaining the topological structure of the framework unchanged.

2.2 Geometry optimization

The structures of the frameworks and the adsorption complexes were optimized in a two-step process. In the first step, the unit cells of the IRMOFs were optimized with full periodic boundary conditions in order to retain the structure stability of IRMOFs. All the framework atoms were set as flexible to adjusted the energetically minimization of the structure. Similar as previous works (Liu et al. 2013; Liu et al. 2012; Mu et al. 2010), the gradient corrected (GGA) correlation functional of Perdew and Wang (PW91) (Perdew and Wang 1992) was employed with the double numerical plus (DNP) polarization basis set (Delley 1990, 1991), carried out by Dmol^3 code (Delley 2000). All electron was employed in the nucleus, the orbital global cutoff quality was set as fine, and the convergence threshold parameters for optimization were 1×10^{-5} for energy.

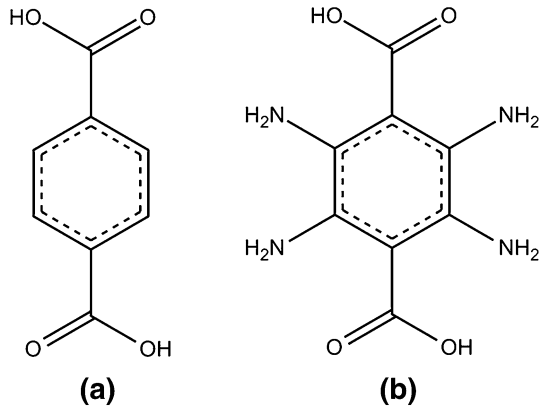

Fig. 2 Organic linkers of IRMOFs: **a** BDC of IRMOF-1 and **b** N_4BDC of IRMOF-NH_2

In the second step, the supercell models of IRMOFs were generated from the optimized unit cell by $1 \times 2 \times 1$ primitive cells to proceed the optimization of the adsorbate-adsorbent complexes, as shown in Fig. 3. This calculation, also using DFT-GGA/PW91 method, was conducted to determine the energy minimum orientations and positions of the adsorbate molecules on the frameworks. Because of large amount of atoms in a unit cell, periodic supercell model was performed, which not only maintains the local environment of the binding sites but also reduces computational demanding. In this step, all the framework atoms were set as fixed to prevent deformations of the structure, while the atoms of adsorbates were allowed to relax in order to satisfy the certain minimum-energy criteria. Previous work (Ford et al. 2009) had indicated the negligible atomic flexibility of IRMOF structures when the kinetic diameters of the adsorbed molecules were greatly smaller than pore size; and/or the frameworks did not sustain any strong guest–host interactions in the adsorption system. The purpose of this step is to relax the energy of the adsorption system and prepare for the following calculations of BEs.

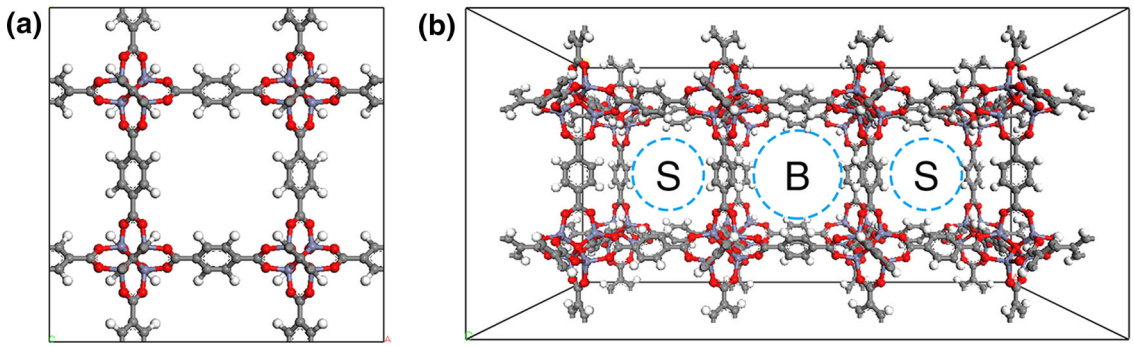

Fig. 1 The **a** crystal structure and **b** the pores division of IRMOF-1 (*S* represents small cells, while *B* represents big cells)

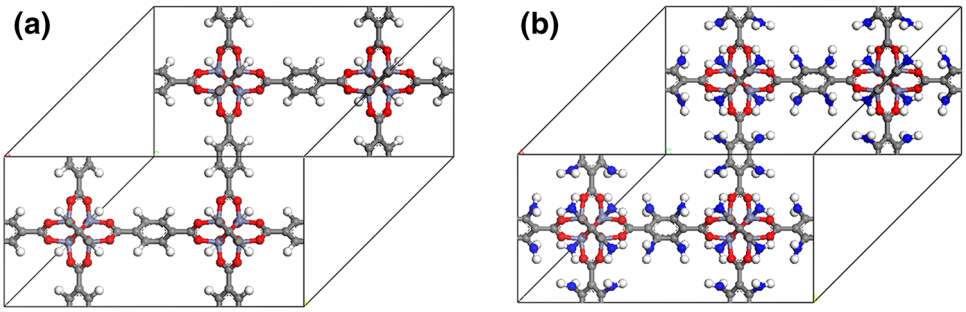

Fig. 3 The supercell models of IRMOFs: **a** IRMOF-1 **b** IRMOF-NH_2

After geometry optimization, a variety of possible configurations were found, but only those in the energy minimum locations (binding sites) were discussed in detail. Four major binding sites, denoted as site IS (small cell of the metal corner), site IB (big cell of the metal corner), site IIS (small cell of the linker), site IIB (big cell of the linker), respectively, were discussed. In addition, two types of orientations of VOC molecules on each binding site, *cis*-form orientation (the oxygen atoms of VOCs turn to the binding sites, noted as 1) and anti-form orientation (–CH_3 groups turn to the binding sites, noted as 2), were also taken into account, as shown in Fig. 4. Thus, eight (4 × 2) adsorption configurations were considered in this work.

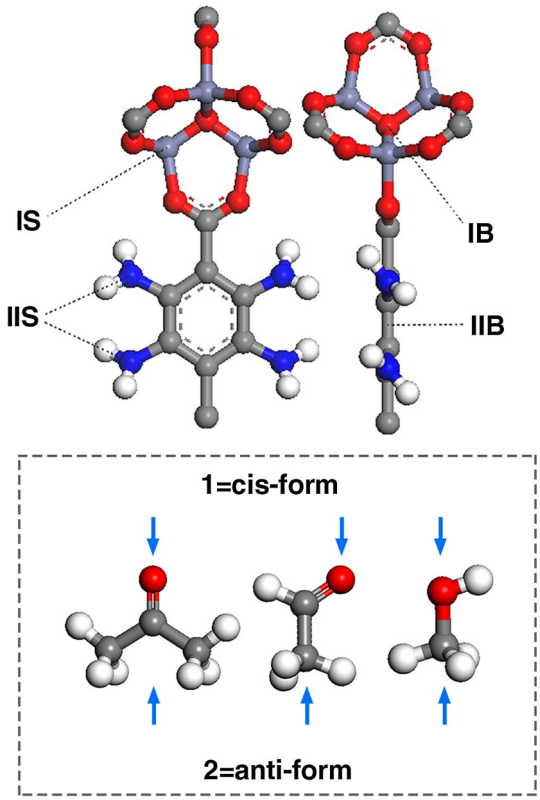

Fig. 4 The binding sites in IRMOFs and the orientation of VOCs to the binding sites. *IS* the small cell at the corner, *IB* the big cell at the corner, *IIS* the small cell at the linker, *IIB* the big cell at the linker. *1* represents the *cis*-form orientation of adsorbates, while *2* represents the anti-form orientation

2.3 Binding energies calculations

BE is regarded as a significant parameter in indicating the interaction strength of adsorbate adsorption on MOFs, hence the BE calculations of the selected adsorption configurations were processed after geometry optimization, also using GGA-level of PW91/DNP procedure. Only one VOC molecule per supercell was considered and the BE was evaluated as Eq. 1:

$$BE = E_{MOF/VOC} - (E_{MOF} + E_{VOC}) \quad (1)$$

where $E_{MOF/VOC}$ is the total energy of the IRMOFs/VOCs adsorption complexes in equilibrium state, and E_{MOF} and E_{VOC} are the total energy of the guest-free IRMOFs structures and the chosen VOC adsorbate, respectively. The negative value of binding energy shows the exothermic binding of the VOC adsorbates on IRMOFs, a higher absolute value of BE indicates a stronger adsorption strength.

The chosen functional PW91, combining with DNP basis set, has been successfully used by researchers for geometry optimization and BE calculations of H-bonding and electrostatic-dominated interactions on MOFs (Wu et al. 2010; Venkataramanan et al. 2009). Nevertheless, GGA/PW91 simulations have somewhat limitation in describing dispersion energies effects (Pakarinen et al. 2009; Wu et al. 2001), and may slightly underestimates the absolute values of BEs when treating long-range interactions. However, the purpose of this work is to study the role of amino-functionalization on VOC adsorptions by comparing the calculated BEs among the different configurations, and between different adsorption sites. It has been reported that the adsorbate-framework dispersive interactions on IRMOF-1 and IRMOF-NH_2 were comparative, and the amino introduction did not have significant effects on it (Mu et al. 2010). Moreover, the previous work (Torrisi et al. 2009) also indicated a good agreement between PW91 and MP2 method in calculating the BE and configuration of benzene/CO_2 molecular complex, which

was governed by weak van der Waals interactions. It is, therefore, the deviation caused by dispersion effects could be offset when making a relative comparison. Actually, the GGA/PW91 simulations have been successfully employed by many researchers to study weak van der Waals (vdW) interactions on MOFs (Yan et al. 2014; Wu et al. 2014b).

2.4 Atomic partial charge calculations

The atomic partial charges of IRMOFs were computed to quantitatively clarify the amino-functionality effects on charge transfer and ESP of the frameworks. Similar as the previous works (Xu and Zhong 2010; Wu et al. 2012; Priya et al. 2014), the nonperiodic cluster models were used to calculate the ESP derived charges of the atoms in the frameworks, which were treated as the atomic partial charges in this paper. The cluster models were illustrated in Fig. 5. To maintain the correct hybridization, the dangling bonds on the fragmented clusters were terminated by methyl ($–CH_3$) groups. On the basis of the ChelpG method (Breneman and Wiberg 1990), DFT calculations were performed by using unrestricted B3LYP functional. The basis set LANL2DZ was used for metal atom Zn, while 6-31+G* (Hariharan and Pople 1972) was used for the rest of the atoms. For complexes involving heavy metal atoms, the approach of effective core potential basis set (e.g. LANL2DZ) for heavy atoms was commonly adopted to mixed with all-electron basis sets for rest atoms. LANL2DZ is a collection of double-ξ basis sets (Foguet Albiol et al. 2005) that contains effective pseudopotentials to represent the core potential for valence electrons, which can significantly reduce the computational cost. These calculations were performed using the GAUSSIAN 09 suite of programs (Frisch et al. 2009), and the results were listed in Table 1.

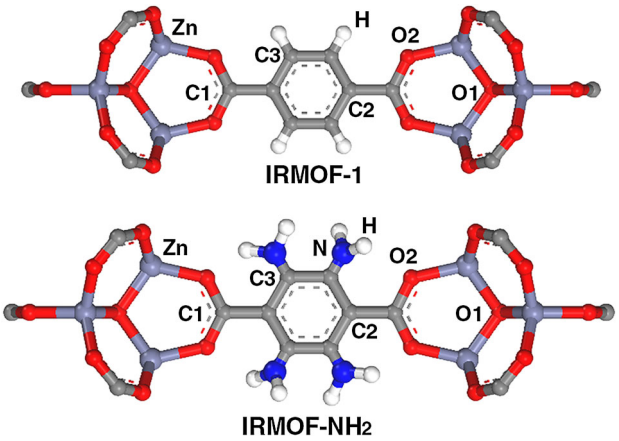

Fig. 5 Cluster models used in the atomic partial charges calculations for IRMOF-1 and IRMOF-NH_2

Table 1 The atomic partial charges (eV) of IRMOFs

Atom types	IRMOF-1	IRMOF-$(NH_2)_4$
C1	+0.73	+1.03
C2	+0.05	−0.52
C3	−0.14	+0.27
H	+0.15	+0.35
N	–	−0.79
O1	−1.53	−2.34
O2	−0.66	−0.86
Zn	+1.28	+1.75

3 Results and discussion

3.1 Electrostatic properties of IRMOFs

Table 1 lists the atomic partial charges of IRMOF-1 and IRMOF-NH_2 (with the atom types denoted in Fig. 5). As can be seen in Table 1, some atomic charges greatly increase after amino-functionalization, e.g. the charges of C3 atoms increase to be +0.27 eV from −0.14 eV, the coordinatively unsaturated site (CUS) of Zn atoms also have a more positive charge of +1.75 eV on IRMOF-NH_2. This indicates an electrons deficit of these atoms that results from the high electronegativity of amino groups. Conversely, the charges on the C2 atoms of IRMOF-NH_2 decrease to a negative one of −0.52 eV from IRMOF-1, and the charges of O1 and O2 atoms also slightly decrease to a more negative value. These results reveal the great influence of the electron-donating groups ($–NH_2$) on the charge distributions of IRMOFs, inducing the electron transfer and electrostatic density redistribution on the whole framework, which may consequently change the VOCs adsorption performance. The detail of amino-functionalization effects on IRMOFs are studied by comparing the BEs in the following sections.

3.2 Adsorption thermodynamics of methanol on IRMOFs

3.2.1 Methanol adsorbed on IRMOF-1

Figure 6 shows the geometric equilibrium configurations and the corresponding BEs on each binding sites of IRMOF-1. It is noted that the BEs of the configurations on site I are significantly higher than those on site II, indicating more adsorption affinity of methanol on CUS sites, which resembles the adsorption of other adsorbates like benzene (Zeng et al. 2012) and small gases (Dubbeldam et al. 2007) on IRMOF-1 verified both experimentally and theoretically. Due to the electronic-accepting effects of CUS sites (Mu et al. 2010), the adsorption on site I is

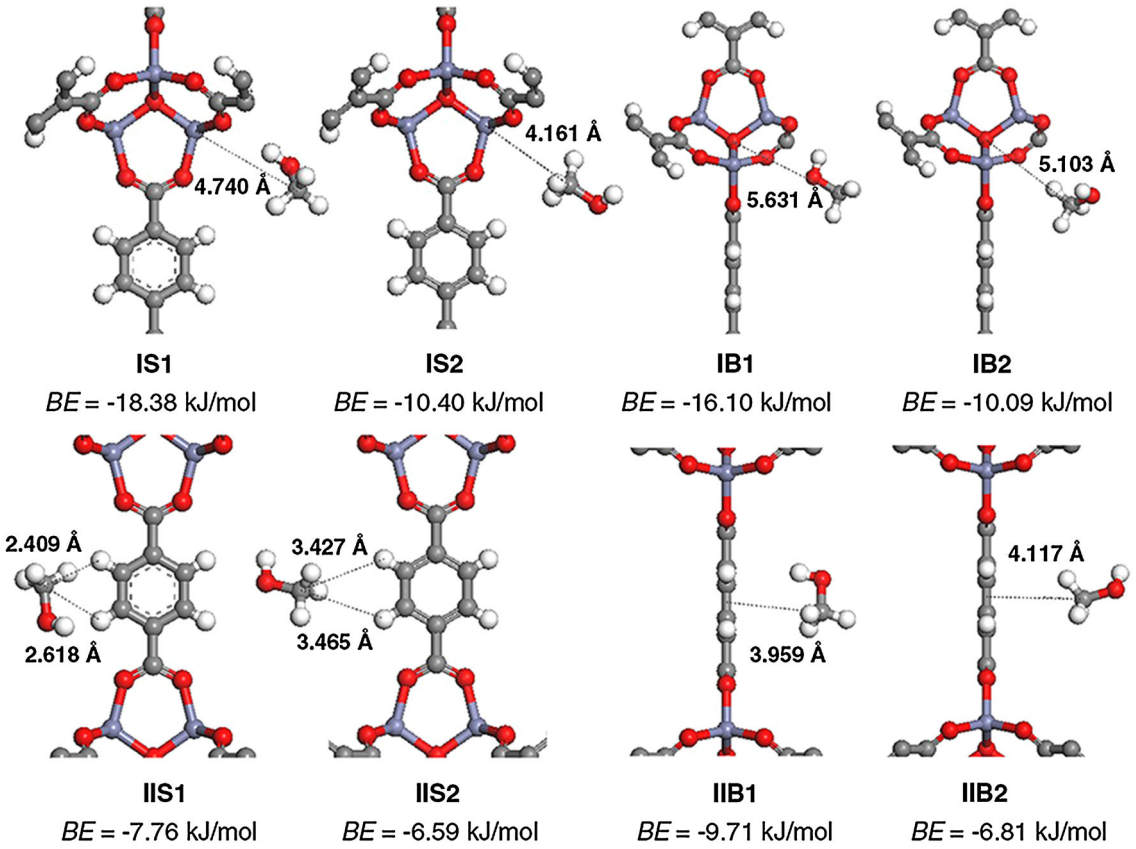

Fig. 6 The DFT optimized configurations and the corresponding BEs in each binding sites of IRMOF-1

governed by electrostatic interactions, which is greatly stronger than the vdW interactions on site II. Besides, the calculated BEs of IRMOF-1 show different trends on site I and site II. The BE on site I follows the order of site IS > site IB, but it turns to be site IIB > site IIS on site II reversely, suggesting varied interaction mechanism on site I and site II.

On site I, larger amount of Zn atoms on the big cell (site IB) give rise to the stronger positive electrostatic field, which will repulsively interacted with adsorbates possessed similar positive field. Contrarily, these adsorbates can attractively interact with site IS, which exhibits relatively weaker positive ESP. It is noted that the BEs of methanol on site IB are weaker than site IS (e.g. −16.10 and 18.38 kJ/mol for IB1 and IS1, respectively), suggesting site IB may repulsively interacts with $–CH_3$ group of methanol, since the $–CH_3$ group possesses positive electrostatic field because of the electron-donating effects of the –OH group. Correspondingly, $-CH_3$ group of methanol is able to interact with site IS preferably. On site II, however, the adsorption behavior of the framework differs from that on site I. The BEs on site IIB are even slightly higher than site IIS (−9.71 and −7.76 kJ/mol for IIB1 and IIS1, respectively), suggesting a π system-dominated interaction on the organic linker. The conjugated π-system with stronger negative electrostatic field presents above both sides of the linker (site IIB), which interacts with the $–CH_3$ group of methanol preferably, while methyl-linker interaction is weaker at the side of aromatic ring (site IIS) due to the lack of π system delocalization.

On the other hand, the orientation and distance of $–CH_3$ group of methanol to the specific binding site also shows varied trends for site I and site II on IRMOF-1. On both site IS and site IB, methanol with *cis*-form orientation (1) has a greater adsorption affinity (BE) and a farther distance from binding sites than anti-form (2). In this case, the final interaction strength of methanol on site I can be controlled by either the electrostatic-dominated interaction between $–CH_3$ group and binding sites or the steric hindrance of methanol molecule, or both of them, depending on the properties of the adsorbate molecule, such as ESP, textural properties, etc. The behaviors of methanol on site I suggests that the negative steric hindrance effects of $–CH_3$ group is relatively stronger than the electrostatic interaction with binding sites of the framework. In addition, the H-bonding interaction between –OH group of methanol and the neighboring O2 atoms also contributes to methanol adsorption with *cis*-form orientations (H-O2 distance: 2.33 and 2.50 Å for site IS1 and IB1, and O–H–O_2 angles are less than 20° for both sites). H-bonding interaction should

be considered when two conditions are satisfied: the H-bond distance less than 3.5 Å, and the hydrogen-donor–acceptor angle less than 30° (Luzar and Chandler 1996). On site II, however, the BEs become more exothermic in a closer binding distance with *cis*-form configuration, e.g. methanol has a greater adsorption affinity on site IIB1 in a closer binding distance (3.959 Å) than site IIB2 (4.117 Å). It suggests the negative steric hindrance effects becomes less important on site II and the adsorption turns to be controlled by methyl-π system interactions, resulting from the larger binding environment around the organic linker than the metal corner.

Combining the adsorption behaviors and the electrostatic properties of methanol and IRMOF-1, a plausible adsorption mechanism is deduced that the adsorption of methanol on IRMOF-1 is likely dominated by the electrostatic interactions between the binding sites and the $–CH_3$ group of methanol, while the polar group (–OH) of methanol only interacts with the framework through H-bonding interactions. This will be further verified with the comparative study of aldehyde and acetone in the following section.

3.3 Methanol adsorbed on IRMOF-NH_2

In order to understand the interaction mechanism of methanol over IRMOFs, electron-donating $–NH_3$ groups are introduced to modify the electrostatic properties of the framework for comparison. The adsorption configurations and the corresponding BEs on each binding sites of IRMOF-NH_2 are calculated in Fig. 7. As have discussed earlier, amino-functionalization has a great influence on the charge distribution of the framework, which is expected to improve methanol adsorption performance, similar as the adsorption of CO_2 (Mu et al. 2010) on amino-modified IRMOFs. The BEs on site II are indeed greatly intensified by $–NH_2$ groups, especially on site IIS1 and IIB1 (13.12 and 7.57 kJ/mol higher than IRMOF-1, respectively). Besides, methanol tends to stabilize in a closer binding distance with *cis*-form orientation on site II, similar as IRMOF-1, indicating amino-functionality does not significantly change the steric environment around the linker, since the site II interaction on IRMOF-NH_2 is still dominated by π system. However, the BEs on site I (site IS1/2 and IB1/2) of IRMOF-NH_2 are less exothermic compared to IRMOF-1. It suggests varied effects of amino-functionalization that both enhance the methyl-π system interactions on site II and weaken the interaction strength on site I.

To investigate the varied effects of amino-functionalization on site I and site II, the contour maps of the ESPs of IRMOFs are further calculated in Fig. 8. Similar as the previous work (Mu et al. 2010), the ESPs are obtained using BLYP exchange–correlation functional of GGA level, and DNP basis set is also adopted. As shown in Fig. 8, IRMOF-NH_2 has an ESP with larger gradient and higher absolute values above the two sides of the aromatic ring, suggesting a stronger electrostatic field on site II of

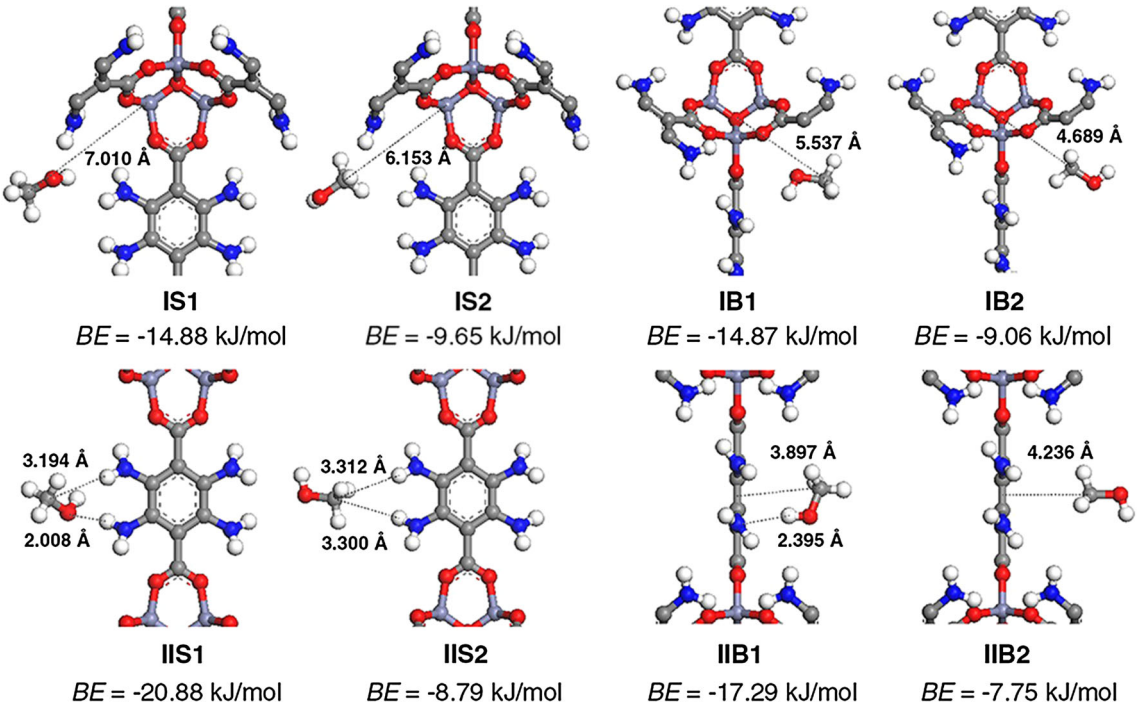

Fig. 7 The DFT optimized configurations and the corresponding BEs in each binding sites of IRMOF-NH_2

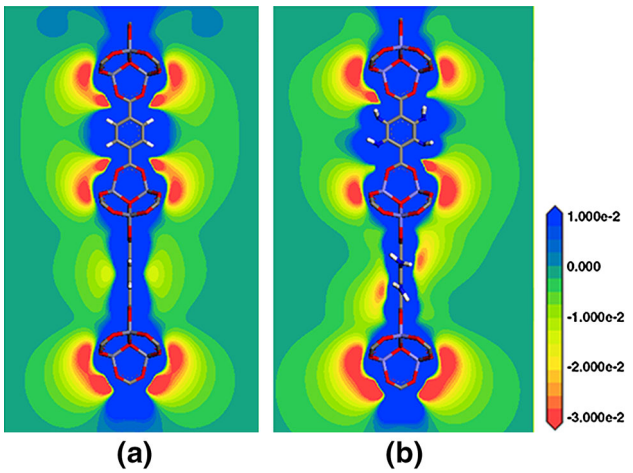

Fig. 8 The contour maps of electrostatic potentials (ESP) for: **a** IRMOF-1 and **b** IRMOF-NH_2

IRMOF-NH_2 than that on IRMOF-1. It can be attributed to the conjugation effect of the lone pair electrons in –NH_2 groups, which greatly enhances the π system delocalization and polarized electron density above the aromatic ring. This observation agrees well with the results for the stronger BEs on site II of IRMOF-NH_2 than IRMOF-1 (shown in Figs. 6, 7). Meanwhile, weak H-bonding interaction between –OH group of methanol and -NH_2 groups forms when these two groups approach each other, which also contributes to adsorbate-adsorbent interactions in addition to the electrostatic interactions. Contrary to site II, the BEs of site I in IRMOF-NH_2 are even slightly weaker compared to IRMOF-1 (shown in Figs. 6, 7). It can be readily evidenced by the increased positive electrostatic fields around the CUS of Zn atoms (as shown in Fig. 8), also as noted from the more positive atomic partial charges of Zn atoms [+0.47 eV higher than IRMOF-1 (from +1.28 eV to +1.75 eV)], indicating adsorbate-adsorbent interactions are suppressed by the repulsive methyl-CUS interactions. Moreover, the negative steric effect of inserted –NH_2 groups also more hinders the adsorption on site I than site II, since the CUS binding sites represent only a small region of the framework and can be easily blocked by the functional groups. Consequently, the adsorption of methanol on site I of IRMOF-NH_2 is strongly suppressed by both the electrostatically repulsive interaction and the steric inhibition of –NH_2 groups.

3.4 Adsorption thermodynamics of aldehyde and acetone on IRMOFs

3.4.1 Aldehyde and acetone adsorbed on IRMOF-1

To verify the electrostatic-dominated interaction mechanism between –CH_3 group of the adsorbate and binding sites of the framework, the adsorption of aldehyde and acetone with electron-withdrawing groups (–CHO and –C=O) on IRMOFs are performed for comparative study in Fig. 9. Similar as methanol on IRMOF-1, both aldehyde and acetone tend to be stabilized with *cis*-form orientation, and prefer site I than site II. Nevertheless, the BEs of both these two adsorbates follow the order: site IB >site IS on site I and site IIS >site IIB on site II, contradictory with the adsorption behaviors of methanol. The –CH_3 groups of aldehyde and acetone exhibit negative ESP because of the electron-withdrawing effects of their polar groups (–CHO for aldehyde and –C=O for acetone, respectively), resulting in the electrostatically inter-attractive interactions with site IB and site IIS. The observation also supports the plausible interaction mechanism we have discussed, suggesting the adsorption is governed by methyl-binding site interactions. In addition, the BEs of acetone on all the binding sites are slightly more exothermic than aldehyde, indicating a stronger electron-withdrawing ability of –C=O group than –CHO group.

3.5 Aldehyde and acetone adsorbed on IRMOF-NH_2

The adsorption of aldehyde and acetone on IRMOF-NH_2 is also performed for a further investigation, as the calculated BEs shown in Fig. 10. As is expected, aldehyde and acetone have stronger BEs on site I of IRNMOF-NH_2 compared to IRMOF-1, resulting from the enhanced positive ESP around the metal corners by amino-functionalization. Meanwhile, the increased BEs are slightly higher on site IB than site IS for IRMOF-NH_2 (e.g. for aldehyde, 2.48 and 0.91 kJ/mol higher than IRMOF-1 on site IB1 and IS1, respectively), implying the enhanced effect of amino-functionalization on site IB is greater than site IS.

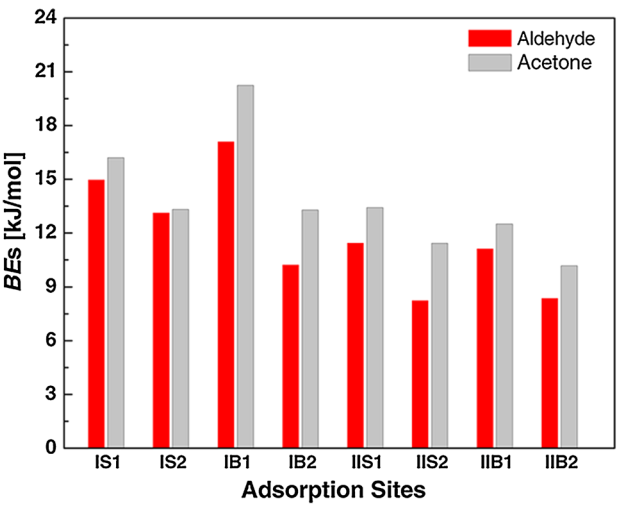

Fig. 9 The BEs of aldehyde, acetone and methanol adsorbed in IRMOF-1

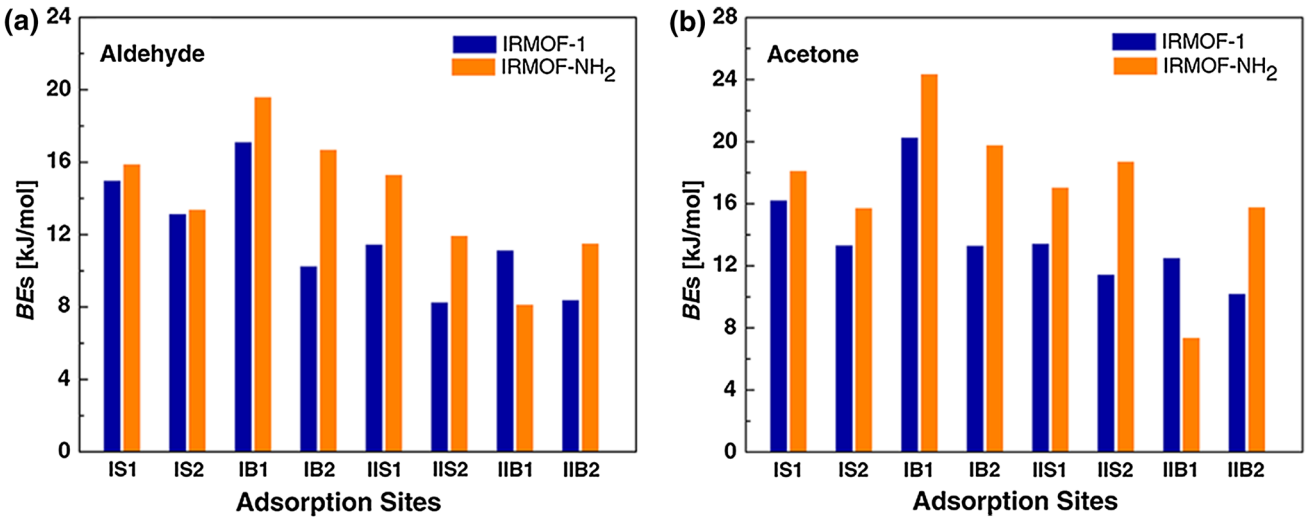

Fig. 10 The binding energies of **a** aldehyde and **b** acetone adsorbed in IRMOF-1 and IRMOF-NH_2

Additionally, the BEs of aldehyde and acetone on site IIS1/2 are also stronger than IRMOF-1, suggesting the relatively stronger positive potential field of site IIS to attractively interact with the negative potential $–CH_3$ group, which results from greatly enhanced delocalization of π system above the aromatic ring (shown in Fig. 8b).

On the basis of the interaction mechanism deduced, the adsorption of aldehyde and acetone on both site IIB1 and site IIB2 of IRMOF-NH_2 are expected and should be hindered by amino-insertion, resulting from the repulsive electrostatic interactions between $–CH_3$ group and the enhanced π system on site IIB, similar to the repulsive adsorption of methanol on site I of IRMOF-NH_2. However, it is interesting to find the exception on site IIB2, where the BEs of both aldehyde and acetone are unexpectedly more exothermic compared to IRMOF-1. As illustrated in Fig. 11, $–CH_3$ groups of the adsorbates on site IIB have greater adsorption affinity with anti-form orientation (site IIB2), which also has a closer distance from the binding site than *cis*-form (site IIB1) (1.57 and 2.05 Å closer for aldehyde and acetone, respectively). Figure 8b shows positive potential field exists between the aromatic ring and the π delocalization region, as confirmed from the positive partial charges of aromatic C3 atoms (increased to +0.27 eV from −0.14 eV of IRMOF-1), which is likely to interact with $–CH_3$ groups of aldehyde and acetone preferably when approaching close enough. Compared to methanol, $–CH_3$ groups of aldehyde and acetone possess stronger ESP and therefore, is capable of accessing the opposite electrostatic binding site via the negative π system delocalization. These adsorption behaviors of aldehyde and acetone on site IIB2 show the interaction of VOCs with MOFs is complex and that more work is needed to probe the mechanisms of these processes. In addition, acetone is observed to have a slightly weaker adsorption affinity (−7.35 kJ/mol) than aldehyde (−8.12 kJ/mol) on site IIB1 of IRMOF-NH_2. It can attribute to $–CH_3$ groups of acetone

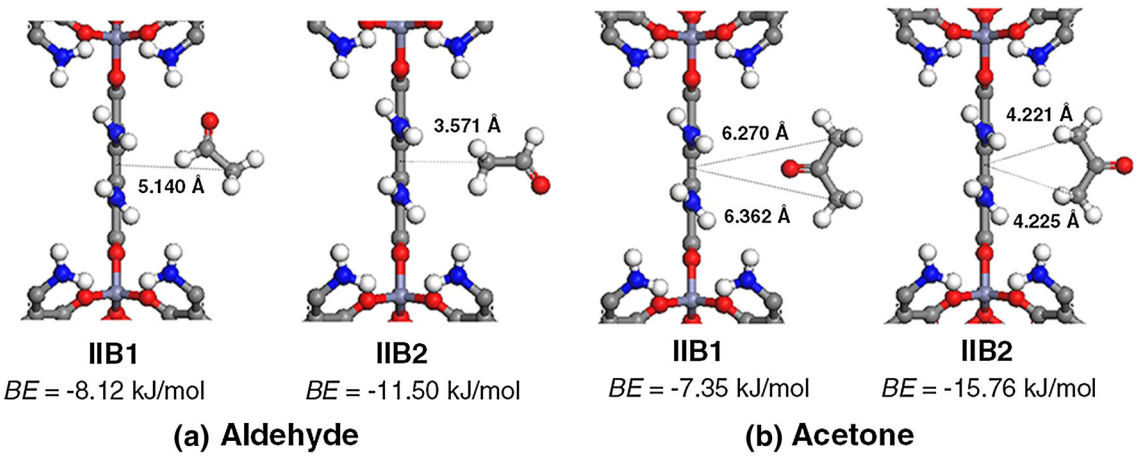

Fig. 11 The DFT optimized structures of **a** aldehyde and **b** acetone in site IIB of IRMOF-NH_2

that possesses both stronger negative electrostatic field and a larger steric occupation than aldehyde, inducing the repulsive electrostatic interactions and negative steric hindrance effects on site IIB1, and consequently weaken the adsorbate-adsorbent interactions.

4 Conclusions

DFT calculation has been carried out to study the adsorption behaviors of methanol, aldehyde and acetone on IRMOFs. The BEs and the energy-minimum configurations of these VOCs on IRMOF-1 and a newly-constructed IRMOF-NH_2, are compared to reveal the functionality effects of amino groups on VOCs adsorption. Moreover, the atomic partial charges and ESPs of IRMOFs are also calculated to elucidate the electron transference and distribution on the frameworks caused by the inserted amino groups. The calculated results indicate that the electron-donating effect of amino groups greatly intensifies both the electrostatic delocalization above two sides of the organic linkers (site II), and the positive potential field around the metal corners (site I). Consequently, the adsorption of methanol is greatly enhanced by attractive interactions on site II of IRMOF-NH_2, but weakened by electrostatically repulsive interactions on site I. However, reverse behaviors are observed on the adsorption of aldehyde and acetone, resulting from the varied ESP field of their methyl groups. A plausible adsorption mechanism is proposed that the adsorption of these VOCs on IRMOFs is likely controlled by electrostatic interaction between methyl groups of the adsorbates and the binding sites of the framework, while the polar groups of these adsorbates only interact with framework through weak interaction strength (e.g. H-bonding). Besides, the inserted amino groups may also sterically hinder the electrostatic interactions, depending on the configurations and the electronic properties of the adsorbates. The underlying binding mechanism elucidated by a detailed electrostatic and structural analysis, provides guidelines to the synthesis of new functional MOFs for the adsorption of VOCs.

Acknowledgments We gratefully acknowledge the financial support from the National Natural Science Foundation of China (Nos. 20936001 and 21176084), the National High Technology Research and Development Program of China (No. 2013AA065005), Guangdong Natural Science Foundation (S2011030001366).

References

Babarao, R., Hu, Z., Jiang, J., Chempath, S., Sandler, S.I.: Storage and separation of CO2 and CH4 in silicalite, C-168 schwarzite, and IRMOF-1: a comparative study from Monte Carlo simulation. Langmuir **23**(2), 659–666 (2007). doi:10.1021/la062289p

Breneman, C.M., Wiberg, K.B.: Determining atom-centered monopoles from molecular electrostatic potentials. The need for high sampling density in formamide conformational analysis. J. Comput. Chem. **11**(3), 361–373 (1990). doi:10.1002/jcc.540110311

Cicmanec, P., Bulanek, R., Frydova, E., Kolarova, M.: Study of thermodynamic characteristics of CO adsorption on Li exchanged zeolites. Adsorpt. J. Int. Adsorpt. Soc. **19**(2–4), 381–389 (2013). doi:10.1007/s10450-012-9461-8

Delley, B.: An all-electron numerical method for solving the local density functional for polyatomic molecules. J. Chem. Phys. **92**(1), 508–517 (1990). doi:10.1063/1.458452

Delley, B.: Analytic energy derivatives in the numerical local-density-functional approach. J. Chem. Phys. **94**(11), 7245–7250 (1991). doi:10.1063/1.460208

Delley, B.: From molecules to solids with the DMol3 approach. J. Chem. Phys. **113**(18), 7756–7764 (2000). doi:10.1063/1.1316015

Devautour-Vinot, S., Maurin, G., Serre, C., Horcajada, P., Paula da Cunha, D., Guillerm, V., de Souza Costa, E., Taulelle, F., Martineau, C.: Structure and dynamics of the functionalized MOF type UiO-66(Zr): NMR and dielectric relaxation spectroscopies coupled with DFT calculations. Chem. Mater. **24**(11), 2168–2177 (2012). doi:10.1021/cm300863c

Dou, B., Hu, Q., Li, J., Qiao, S., Hao, Z.: Adsorption performance of VOCs in ordered mesoporous silicas with different pore structures and surface chemistry. J. Hazard. Mater. **186**(2–3), 1615–1624 (2011). doi:10.1016/j.jhazmat.2010.12.051

Dubbeldam, D., Frost, H., Walton, K.S.: Snurr RQ (2007) Molecular simulation of adsorption sites of light gases in the metal–organic framework IRMOF-1. Fluid Phase Equilibria **261**(1–2), 152–161 (2007). doi:10.1016/j.fluid.2007.07.042

Eddaoudi, M., Kim, J., Rosi, N., Vodak, D., Wachter, J., O'Keeffe, M., Yaghi, O.M.: Systematic design of pore size and functionality in isoreticular MOFs and their application in methane storage. Science **295**(5554), 469–472 (2002). doi:10.1126/science.1067208

Fang, H., Demir, H., Kamakoti, P., Sholl, D.S.: Recent developments in first-principles force fields for molecules in nanoporous materials. J. Mater. Chem. A **2**(2), 274–291 (2014). doi:10.1039/C3TA13073H

Ferey, G., Mellot, D.C., Serre, C., Millange, F.: Crystallized frameworks with giant pores: are there limits to the possible? Acc. Chem. Res. **38**(4), 217–225 (2005). doi:10.1021/ar040163i

Foguet Albiol, D., O'Brien, T.A., Wernsdorfer, W., Moulton, B., Zaworotko, M.J., Abboud, K.A., Christou, G.: DFT computational rationalization of an unusual spin ground state in an Mn-12 single-molecule magnet with a low-symmetry loop structure. Angew. Chem. Int. Ed. **44**(6), 897–901 (2005). doi:10.1002/anie.200461820

Ford, D.C., Dubbeldam, D., Snurr, R.Q.: The effect of framework flexibility on diffusion of small molecules in the metal–organic framework IRMOF-1. Diffus. Fundam. **11**(78), 1–8 (2009)

Frisch, M.J., Trucks, G.W., Schlegel, H.B.: Gaussian 09, revision D. 01. Gaussian Inc, Wallingford (2009)

Furukawa, H., Cordova, K.E., O'Keeffe, M., Yaghi, O.M.: The chemistry and applications of metal–organic frameworks. Science **341**(6149), 1230444 (2013). doi:10.1126/science.1230444

Hariharan, P.C., Pople, J.A.: The effect of d-functions on molecular orbital energies for hydrocarbons. Chem. Phys. Lett. **16**(2), 217–219 (1972). doi:10.1016/0009-2614(72)80259-8

Hu, Z., Chen, Y., Jiang, J.: Liquid chromatographic separation in metal–organic framework MIL-101: a molecular simulation study. Langmuir **29**(5), 1650–1656 (2013). doi:10.1021/la3045972

Kim, K.J., Ahn, H.G.: The effect of pore structure of zeolite on the adsorption of VOCs and their desorption properties by

microwave heating. Microporous Mesoporous Mater. **152**, 78–83 (2012). doi:10.1016/j.micromeso.2011.11.051

Laaksonen, A., Hienola, J., Kulmala, M., Arnold, F.: Supercooled cirrus cloud formation modified by nitric acid pollution of the upper troposphere. Geophys. Res. Lett. **24**(23), 3009–3012 (1997). doi:10.1029/97gl02996

Le Cloirec, P.: Adsorption onto activated carbon fiber cloth and electrothermal desorption of volatile organic compound (VOCs): a specific review. Chin. J. Chem. Eng. **20**(3), 461–468 (2012)

Leus, K., Couck, S., Vandichel, M., Vanhaelewyn, G., Liu, Y–.Y., Marin, G.B., Driessche, I.V., Depla, D., Waroquier, M., Speybroeck, V.V., Denayer, J.F.M., Voort, P.V.D.: Synthesis, characterization and sorption properties of NH2-MIL-47. Phys. Chem. Chem. Phys. **14**(44), 15562–15570 (2012). doi:10.1039/C2CP42137B

Liang, Z., Marshall, M., Chaffee, A.L.: Comparison of Cu-BTC and zeolite 13X for adsorbent based CO_2 separation. Energy Procedia **1**(1), 1265–1271 (2009). doi:10.1016/j.egypro.2009.01.166

Lin, K.-S., Adhikari, A.K., Su, Y.-H., Shu, C.-W., Chan, H.-Y.: Synthesis, characterization, and hydrogen storage study by hydrogen spillover of MIL-101 metal organic frameworks. Adsorpt. J. Int. Adsorpt. Soc. **18**(5–6), 483–491 (2012). doi:10.1007/s10450-012-9438-7

Liu, D.F., Wu, Y.B., Xia, Q.B., Li, Z., Xi, H.X.: Experimental and molecular simulation studies of CO_2 adsorption on zeolitic imidazolate frameworks: ZIF-8 and amine-modified ZIF-8. Adsorpt. J. Int. Adsorpt. Soc. **19**(1), 25–37 (2013). doi:10.1007/s10450-012-9407-1

Liu, J., Cheney, M.A., Wu, F., Li, M.: Effects of chemical functional groups on elemental mercury adsorption on carbonaceous surfaces. J. Hazard. Mater. **186**(1), 108–113 (2011). doi:10.1016/j.jhazmat.2010.10.089

Liu, Y., Liu, J., Chang, M., Zheng, C.G.: Effect of functionalized linker on CO_2 binding in zeolitic imidazolate frameworks: density functional theory study. J. Phys. Chem. C **116**(32), 16985–16991 (2012). doi:10.1021/jp302619m

Luebbers, M.T., Wu, T., Shen, L., Masel, R.I.: Trends in the adsorption of volatile organic compounds in a large-pore metal–organic framework, IRMOF-1. Langmuir **26**(13), 11319–11329 (2010). doi:10.1021/la100635r

Luzar, A., Chandler, D.: Hydrogen-bond kinetics in liquid water. Nature **379**(6560), 55–57 (1996)

Mayo, S.L., Olafson, B.D., Goddard, W.A.: DREIDING: a generic force field for molecular simulations. J. Phys. Chem. **94**(26), 8897–8909 (1990). doi:10.1021/j100389a010

Montoro, C., Linares, F., Procopio, E.Q., Senkovska, I., Kaskel, S., Galli, S., Masciocchi, N., Barea, E., Navarro, J.A.R.: Capture of nerve agents and mustard gas analogues by hydrophobic robust MOF-5 type metal–organic frameworks. J. Am. Chem. Soc. **133**(31), 11888–11891 (2011). doi:10.1021/ja2042113

Mu, W., Liu, D.H., Yang, Q.Y., Zhong, C.L.: Computational study of the effect of organic linkers on natural gas upgrading in metal–organic frameworks. Microporous Mesoporous Mater. **130**(1–3), 76–82 (2010). doi:10.1016/j.micromeso.2009.10.015

Pakarinen, O.H., Mativetsky, J.M., Gulans, A., Puska, M.J., Foster, A.S., Grutter, P.: Role of van der Waals forces in the adsorption and diffusion of organic molecules on an insulating surface. Phys. Rev. B **80**(8), 085401 (2009)

Perdew, J.P., Wang, Y.: Accurate and simple analytic representation of the electron-gas correlation energy. Phys. Rev. B **45**(23), 13244–13249 (1992)

Priya, A.M., Senthilkumar, L., Kolandaivel, P.: Hydrogen-bonded complexes of serotonin with methanol and ethanol: a DFT study. Struct. Chem. **25**(1), 139–157 (2014). doi:10.1007/s11224-013-0260-y

Rappe, A.K., Casewit, C.J., Colwell, K.S., Goddard, W.A., Skiff, W.M.: UFF, a full periodic table force field for molecular mechanics and molecular dynamics simulations. J. Am. Chem. Soc. **114**(25), 10024–10035 (1992). doi:10.1021/ja00051a040

Su, F.C., Mukherjee, B., Batterman, S.: Determinants of personal, indoor and outdoor VOC concentrations: an analysis of the RIOPA data. Environ. Res. **126**, 192–203 (2013). doi:10.1016/j.envres.2013.08.005

Torrisi, A., Bell, R.G., Mellot-Draznieks, C.: Predicting the impact of functionalized ligands on CO_2 adsorption in MOFs: a combined DFT and grand canonical Monte Carlo study. Microporous Mesoporous Mater. **168**, 225–238 (2013). doi:10.1016/j.micromeso.2012.10.002

Torrisi, A., Mellot-Draznieks, C., Bell, R.G.: Impact of ligands on CO_2 adsorption in metal–organic frameworks: First principles study of the interaction of CO_2 with functionalized benzenes. I. Inductive effects on the aromatic ring. J. Chem. Phys. **130**(19), 194703 (2009). doi:10.1063/1.3120909

Venkataramanan, N.S., Sahara, R., Mizuseki, H., Kawazoe, Y.: Probing the structure, stability and hydrogen adsorption of lithium functionalized isoreticular MOF-5 (Fe, Cu Co, Ni and Zn) by density functional theory. Int. J. Mol. Sci. **10**(4), 1601–1608 (2009)

Wolkoff, P.: Indoor air pollutants in office environments: assessment of comfort, health, and performance. Int. J. Hyg. Environ. Health **216**(4), 371–394 (2013). doi:10.1016/j.ijheh.2012.08.001

Wu, D., Maurin, G., Yang, Q., Serre, C., Jobic, H., Zhong, C.: Computational exploration of a Zr-carboxylate based metal–organic framework as a membrane material for CO_2 capture. J. Mater. Chem. A **2**(6), 1657–1661 (2014a). doi:10.1039/C3TA13651E

Wu, D., Yang, Q., Zhong, C., Liu, D., Huang, H., Zhang, W., Maurin, G.: Revealing the structure–property relationships of metal–organic frameworks for CO_2 capture from flue gas. Langmuir **28**(33), 12094–12099 (2012). doi:10.1021/la302223m

Wu, H., Simmons, J.M., Srinivas, G., Zhou, W., Yildirim, T.: Adsorption sites and binding nature of CO_2 in prototypical metal–organic frameworks: a combined neutron diffraction and first-principles study. J. Phys. Chem. Lett. **1**(13), 1946–1951 (2010). doi:10.1021/jz100558r

Wu, L., Xiao, J., Wu, Y., Xian, S., Miao, G., Wang, H., Li, Z.: A combined experimental/computational study on the adsorption of organosulfur compounds over metal–organic frameworks from fuels. Langmuir **30**(4), 1080–1088 (2014b). doi:10.1021/la404540j

Wu, X., Vargas, M.C., Nayak, S., Lotrich, V., Scoles, G.: Towards extending the applicability of density functional theory to weakly bound systems. J. Chem. Phys. **115**(19), 8748–8757 (2001). doi:10.1063/1.1412004

Xu, Q., Zhong, C.: A general approach for estimating framework charges in metal–organic frameworks. J. Phys. Chem. C **114**(11), 5035–5042 (2010). doi:10.1021/jp910522h

Xuemin, H., Fangning, F., Li, C.: The competitive adsorption of multi-component VOCs on activated carbon. In: International Conference on Electric Technology and Civil Engineering (ICETCE), pp. 1669–1672 (2011)

Yaghi, O.M., O'Keeffe, M., Ockwig, N.W., Chae, H.K., Eddaoudi, M., Kim, J.: Reticular synthesis and the design of new materials. Nature **423**(6941), 705–714 (2003). doi:10.1038/nature01650

Yan, D., Tang, Y., Lin, H., Wang, D.: Tunable two-color luminescence and host-guest energy transfer of fluorescent chromophores encapsulated in metal–organic frameworks. Sci. Rep. (2014). doi:10.1038/srep04337

Yang, Q., Wiersum, A.D., Llewellyn, P.L., Guillerm, V., Serre, C., Maurin, G.: Functionalizing porous zirconium terephthalate UiO-66(Zr) for natural gas upgrading: a computational

exploration. Chem. Commun. **47**(34), 9603–9605 (2011). doi:10.1039/C1CC13543K

Yang, Y., Chen, H., Ye, C.: EXAFS and DFT studies of microscopic structure with different density upon Zn(II) adsorption on anatase TiO_2. Adsorpt. J. Int. Adsorpt. Soc. **19**(5), 1019–1025 (2013). doi:10.1007/s10450-013-9510-y

Young, D.: Computational chemistry: a practical guide for applying techniques to real world problems. Wiley, New York (2004)

Zeng, Y., Zhu, X., Yuan, Y., Zhang, X., Ju, S.: Molecular simulations for adsorption and separation of thiophene and benzene in Cu-BTC and IRMOF-1 metal–organic frameworks. Sep. Purif. Technol. **95**, 149–156 (2012). doi:10.1016/j.seppur.2012.04.032

Zhang, K., Chen, Y., Nalaparaju, A., Jiang, J.: Functionalized metal–organic framework MIL-101 for CO2 capture: multi-scale modeling from ab initio calculation and molecular simulation to breakthrough prediction. CrystEngComm **15**(47), 10358–10366 (2013). doi:10.1039/c3ce41737a